

The Carboxy-Terminal Tail of Pyruvate Dehydrogenase Kinase 2 Is Required for the Kinase Activity[†]

Alla Klyuyeva, Alina Tuganova, and Kirill M. Popov*

Department of Biochemistry and Molecular Genetics, School of Medicine, University of Alabama, Birmingham, Alabama 35294

Received March 31, 2005; Revised Manuscript Received June 30, 2005

ABSTRACT: Pyruvate dehydrogenase kinase 2 (PDK2) is a prototypical mitochondrial protein kinase that regulates the activity of the pyruvate dehydrogenase complex. Recent structural studies have established that PDK2 consists of a catalytic core built of the B and K domains and the relatively long amino and carboxyl tails of unknown function. Here, we show that the carboxy-terminal truncation variants of PDK2 display a greatly diminished capacity for phosphorylation of holo-PDC. This effect is due largely to the inability of the transacetylase component of PDC to promote the phosphorylation reaction catalyzed by the truncated PDK2 variants. Furthermore, the truncated forms of PDK2 bind poorly to the lipoyl-bearing domain(s) provided by the transacetylase component. Taken together, these data strongly suggest that the carboxyl tails of PDK isozymes contribute to the lipoyl-bearing domain-binding site of the kinase molecule. We also show that the carboxyl tails derived from isozymes PDK1, PDK3, and PDK4 are capable of supporting the kinase activity of the kinase core derived from PDK2 as well as binding of the respective PDK2 chimeras to the lipoyl-bearing domain. Furthermore, the chimera carrying the carboxyl tail of PDK3 displays a stronger response to the addition of the transacetylase component along with a better binding to the lipoyl-bearing domain, suggesting that, at least in part, the differences in the amino acid sequences of the carboxyl tails account for the differences between PDK isozymes.

Mammalian mitochondria harbor four closely related protein kinases (isozymes PDK1–PDK4)¹ that regulate the activity of the pyruvate dehydrogenase complex (PDC) (1–3) and thereby control the disposal rates of pyruvate and of other metabolically related three-carbon compounds (4).

It is generally believed that at least three of the four isozymes (PDK1–PDK3) are the integral components of a multienzyme complex (3, 5). On average, PDC contains just two to three kinase molecules per complex (6). A growing body of evidence strongly suggests that the kinase molecule uses the so-called lipoyl-bearing domains (LBDs) as docking sites for the attachment to the complex (7–9). In PDC, there are three types of LBDs (LBD1–LBD3) (10). Two of those domains (LBD1 and LBD2) are provided by the acetyltransferase component of the complex (E2) (11), and one (LBD3) is provided by the so-called E3-binding protein (E3BP) (12), which is a structural component of PDC tightly integrated

with E2 (E2–E3BP subcomplex) (10). LBD2 is thought to be the primary binding site for the kinase molecule (13). Kinase activities of PDK1 and PDK2 are known to be regulated by NAD⁺/NADH and CoA/acetyl-CoA (2), which indicates that the kinase can sense the oxidation/reduction and acetylation states of the lipoic acid attached to the lipoyl-bearing domain (14, 15). Although PDK isozymes are bound to the acetyltransferase component, they phosphorylate the dehydrogenase components (E1) of the multienzyme complex (16). In PDC, there are approximately 20–30 copies of pyruvate dehydrogenase physically attached to the core made of 60 copies of E2 and 12 copies of E3BP (10). Thus, to phosphorylate all E1s, the kinase must be able to physically move around the E2–E3BP core without losing its grip on the complex (13, 17).

All PDK isozymes phosphorylate E1 strictly on serine residues (18, 19). However, neither of them displays an appreciable sequence similarity to the Ser/Thr-specific protein kinases residing in other cellular compartments (1, 2). Recent structural studies carried out on PDK2 revealed that the kinase domain of PDK2 displays a unique fold that is remarkably different from the fold characteristic of Ser/Thr- and Tyr-specific protein kinases (20). PDK2 consists of two domains almost equal in size, i.e., the amino-terminal domain (B domain) and the carboxy-terminal domain (K domain). The B domain is folded as a four-helix bundle. The K domain is assembled as a mixed α/β sandwich and carries the nucleotide-binding site (20).

Besides K and B domains that form the catalytic core, the kinase molecule also has long amino and carboxyl tails (1, 2). In contrast to K and B domains that are well-defined

[†] This work was supported by Grants GM51262 and DK56898 from the U.S. Public Health Service.

* To whom correspondence should be addressed: Department of Biochemistry and Molecular Genetics, School of Medicine, University of Alabama, KAUL 440A, 720 20th St. S., Birmingham, AL 35294-0024. Telephone: (205) 996-4065. Fax: (205) 934-0758. E-mail: kpopov@uab.edu.

¹ Abbreviations: PDC, pyruvate dehydrogenase complex; PDK, pyruvate dehydrogenase kinase; PDK1–PDK4, isozymes 1–4 of pyruvate dehydrogenase kinase, respectively; E1, pyruvate dehydrogenase component of PDC; E2, dihydrolipoyl acetyltransferase component of PDC; E3, dihydrolipoamide dehydrogenase component of PDC; E3BP, E3-binding protein component of PDC; LBD1, lipoyl-bearing domain 1; LBD2, lipoyl-bearing domain 2; LBD3, lipoyl-bearing domain 3; SDS–PAGE, sodium dodecyl sulfate–polyacrylamide gel electrophoresis; DTT, dithiothreitol; ITC, isothermal titration calorimetry.

in PDK2 structure, the tails appear to be largely disordered, which is indicative of their inherent flexibility (20). The limited order of the amino- and carboxy-terminal tails in free kinase suggests that they might readily change the conformation when kinase binds to the lipoyl-bearing domain(s) and might directly contribute to the lipoyl-bearing domain-binding site of the kinase molecule. This study, therefore, has been undertaken in an effort to examine a potential role of the amino- and carboxy-terminal tails of PDK2 in the kinase activity and regulation.

EXPERIMENTAL PROCEDURES

Plasmids and Strains. Construction of the expression vectors for E1, the E2–E3BP subcomplex, lipoyl-protein ligase A (LPL_A), the GST–LBD2 fusion protein (amino acids Ser 127–Ile 214), His₆-LBD2 (amino acids Ser 127–Ile 214), and PDK1–PDK4 was described elsewhere (2, 9, 12, 18, 21). The fragments of E2 cDNA (11) encoding LBD1, bases 252 (Ser 1) to 573 (Gln 104), and of E3BP cDNA (12) encoding LBD3, bases 168 (Gly 1) to 483 (Arg 107), were made by polymerase chain reaction (PCR) with *Pfu* polymerase (Stratagene, La Jolla, CA) and appropriate cDNAs as templates (11, 12). Amplification primers carried the unique *Bam*HI (upstream primer) and *Eco*RI (downstream primer) restriction sites (GGA TCC AGT CTT CCC CCG CAT CAG AAG and GAA TTC TTA TTG TGG GGT AGG TGC TGC TGA for LBD1, and GGA TCC GGT GAT CCC ATT AAG ATA CTA ATG and GAA TTC TTA GCG AGG CTC TGA AGG TTT TGA for LBD3; positions of *Bam*HI and *Eco*RI sites are underlined). Downstream primers also incorporated the translation termination codons. Respective cDNAs were subcloned in pUC19 (New England Biolabs Inc., Beverly, MA) and sequenced (22). Sequence-verified plasmids were cut with *Bam*HI and *Eco*RI restrictases. The inserts were purified and subcloned between *Bam*HI and *Eco*RI sites of the pGEX-4T-1 vector (Amersham Biosciences Corp., Piscataway, NJ), producing in-frame fusion with vector-encoded glutathione *S*-transferase (GST). For expression experiments, vectors directing synthesis of GST–LBD1 and GST–LBD3 fusion proteins were transformed into calcium-competent BL21(DE3) (Novagen) cells along with the plasmid directing the expression of bacterial LPL_A (9). Double transformants were selected on M9ZB agar supplemented with 200 μ g/mL ampicillin and 40 μ g/mL chloramphenicol.

The cDNAs encoding truncated forms of PDK2 were obtained by PCR using *Pfu* polymerase and PDK2 cDNA (23) as a template. Amplification primers carried the unique *Nde*I (upstream primer) and *Xho*I (downstream primer) restriction sites. Downstream primers also incorporated the translation termination codons. The cDNA fragments were as follows: PDK2_{ΔN16}, bases 46–1224; PDK2_{ΔN25}, bases 73–1224; PDK2_{ΔN33}, bases 97–1224; PDK2_{ΔC395}, bases 25–1185; PDK2_{ΔC386}, bases 25–1158; PDK2_{ΔC380}, bases 25–1140; PDK2_{ΔC373}, bases 25–1119; and PDK2_{ΔC367}, bases 25–1101. Amplified cDNAs were subcloned into the pUC19 vector and sequenced. Sequence-verified plasmids were cut with *Nde*I and *Xho*I restrictases. The cDNAs were subcloned between the *Nde*I and *Xho*I sites of pET-28a (Novagen Inc., Madison, WI), producing in-frame fusion with a vector-encoded sequence of six consecutive histidine residues (His₆ tag). Resulting expression vectors were transformed into

BL21(DE3) cells along with the plasmid directing the synthesis of molecular chaperonins GroEL and GroES (this vector was obtained as a generous gift from A. Gatenby at DuPont Central Research and Development, Wilmington, DE). Double transformants were selected on M9ZB agar supplemented with 40 μ g/mL kanamycin and 40 μ g/mL chloramphenicol.

PDK2 chimeras carrying the carboxy-terminal tails derived from PDK1, PDK3, and PDK4 were constructed as follows. The unique *Stu*I restriction sites were introduced into PDK1–PDK4 cDNAs at bases 1163, 1082, 1075, and 1093, respectively, using silent mutagenesis (24). Mutagenesis was conducted on previously described pPDK1–pPDK4 vectors directing the synthesis of PDKs carrying the amino-terminal His₆ tags (2). The following primers were used: ATC TAT ATT AAG GCC TTG TCA ACG GAG (PDK1), ATC TAT CTG AAG GCC TTG TCC ACG GAC (PDK2), ATT TAT TTG AAG GCC TTG TCA AGT GAG TCA (PDK3), and ATC TAC TTA AAG GCC TTA TCA TCT GAG (PDK4) (positions of the unique *Stu*I site are underlined). Reactions were set up using the ExSite site-directed mutagenesis kit (Stratagene) essentially as recommended by the manufacturer. The presence of mutations and the fidelity of the rest of the DNAs were confirmed by sequencing (22). Mutagenized plasmids were cut with *Nde*I and *Stu*I restrictases, and arms of pPDK1, pPDK3, and pPDK4 vectors and an insert derived from the pPDK2 vector were isolated. The resulting PDK2 cDNA was ligated into the arms of pPDK1, pPDK3, and pPDK4 vectors, producing plasmids encoding PDK2 chimeras. For expression experiments, these vectors were cotransformed with the pGroESL vector into BL21(DE3) cells.

Protein Expression and Purification. General conditions for the expression of wild-type PDC, E1, the E2–E3BP subcomplex, PDK2, His₆-LBD2, and the GST–LBD2 fusion protein were described previously (2, 9, 12, 18, 21). PDK2 carrying various deletions and PDK2 chimeras were expressed following the established protocol (2). Briefly, the respective expression clones were inoculated into 1 L of M9ZB medium supplemented with 40 μ g/mL kanamycin and 40 μ g/mL chloramphenicol. Cultures were grown at 37 °C with continuous shaking at 200 rpm until the OD at 600 nm reached approximately 0.6. Cultures were cooled on ice and transferred into a shaker–incubator set at 200 rpm, at 16 °C. Expression was induced with isopropyl β -D-thiogalactopyranoside (IPTG) at a final concentration of 0.4 mM for 18 h. Cells were harvested by centrifugation at 5000 rpm (JA-10 rotor) for 30 min at 4 °C. GST–LBD1 and GST–LBD3 fusion proteins were expressed in a similar fashion except that they were expressed in M9ZB medium supplemented with ampicillin and chloramphenicol (each added to final concentrations of 100 and 40 μ g/mL, respectively), and cultures received lipoic acid (0.2 mM) prior to the induction with IPTG.

Purification of wild-type PDC, E1, the E2–E3BP subcomplex, PDK1–PDK4, His₆-LBD2, and the GST–LBD2 fusion protein was described elsewhere (2, 9, 12, 18, 21). Truncated variants of PDK2 and PDK2 chimeras carrying the amino-terminal His₆ tags were purified using TALON metal affinity resin (Clontech Laboratories, Inc., Palo Alto, CA) essentially as described for His₆-PDK2 (2). GST–LBD1 and GST–LBD3 constructs were isolated on glutathione–

Sephacryl 4B beads (Amersham Biosciences, Piscataway, NJ) essentially as described for the GST-LBD2 construct (21). The protein composition of each protein preparation was evaluated by SDS-PAGE analysis. Gels were stained with Coomassie R250. All preparations used in this study were more than 90% pure. The extent of lipoylation of LBD1-LBD3 was examined following the procedure described by Quinn and colleagues (25); their lipoate content was greater than 90%.

PDK2 Activity Assay. The PDK2 activity assay was described previously (2). Reactions were set up at 37 °C in a final volume of 50 μ L containing 20 mM Tris-HCl (pH 7.8), 5 mM MgCl₂, 50 mM KCl, 5 mM DTT, 0.54 mg/mL E1, 0.46 mg/mL E2-E3BP, 0.5 unit/mL E3, 20 μ g/mL kinase, and 0.2 mM [γ -³²P]ATP (specific radioactivity of 100–200 cpm/pmol). Phosphorylation was initiated by the addition of ATP in a volume of 1/10 of the total reaction volume. After incubation for 30 s, 40 μ L aliquots were quenched on Whatman 3MM filters presoaked in a solution of 20% (w/v) trichloroacetic acid, 50 mM sodium pyrophosphate, and 50 mM ATP. After extensive washing, the protein-bound radioactivity was determined by liquid scintillation counting. A negative control (without PDK2) was used to determine the level of nonspecific incorporation. All assays were conducted in triplicate. Activities are reported as means \pm the standard deviation for three to five independent determinations.

PDC Binding Assay. Binding of PDK2 to PDC was assayed essentially as described previously (26). Briefly, binding reactions (100 μ L) were set up in 20 mM Tris-HCl (pH 7.8), 5 mM MgCl₂, 50 mM KCl, and 5 mM DTT. PDC was used at a final concentration of 1.0 mg/mL. The concentration of PDK2 in the binding mixture varied from 0.2 to 2.0 μ M. Samples were incubated for 15 min at room temperature and then loaded onto a 1 mL Sephacryl S-300 column (Amersham Biosciences Corp.) equilibrated in 20 mM Tris-HCl (pH 7.8), 5 mM MgCl₂, 50 mM KCl, 1 mM DTT, and 0.1% (w/v) Tween 20. Prior to the experiment, columns were centrifuged at 900g for 3 min in an IEC Centra CL2 centrifuge (International Equipment Co., Needham Heights, MA) equipped with a bucket rotor. Immediately after being loaded, the columns were centrifuged again at 900g for 3 min. The flow-through containing the complex-bound kinase was analyzed for PDK2 content using Western blot analysis with anti-His₆ tag antibodies. PDK2 incubated alone and treated like other samples was included in all the experiments as a control.

PDK2 Pull-Down Experiment with the GST-LBD2 Construct. Pull-down experiments were carried out as follows: 50 μ L of a 50% (v/v) slurry of glutathione-Sepharose beads in phosphate-buffered saline (PBS) was placed in a Spin-X microcentrifuge filter device with a pore diameter of 0.22 μ m (Corning Inc., Corning, NY). Excess PBS was removed by centrifugation at 6000g for 1 min. Beads were washed three times with 0.5 mL of buffer A [25 mM Tris-HCl (pH 8.0), 0.1 mM EDTA, 2.5 mM MgCl₂, 0.1 M KCl, 5 mM DTT, and 1% (v/v) glycerol]. Equilibrated beads were incubated with 0.4 mL of the GST-LBD2 construct (0.5 mg/mL) in buffer A for 10 min at room temperature. Decorated beads were washed three times with 0.5 mL of buffer A and mixed with 0.4 mL of PDK2 (0.1 mg/mL) made in buffer A. Binding was allowed to proceed for 5–10 min

at room temperature. Unbound PDK2 was removed by centrifugation at 6000g for 1 min followed by three consecutive washes in buffer A (0.5 mL per wash). To elute bound proteins, 0.4 mL of buffer A containing 10 mM reduced glutathione was added to the beads for 10 min at room temperature followed by centrifugation at 6000g for 1 min. Free and bound PDK2 were analyzed using SDS-PAGE. Gels were stained with Coomassie R250. Stained gels were analyzed by scanning densitometry. Scans were quantified using the UN-SCAN-IT automated digitizing system (Silk Scientific, Inc., Orem, UT). After normalization for the amount of GST-LBD2 construct, data were expressed as a percent of control. Pull-down of PDK2 on GST-LBD1 and GST-LBD3 constructs, as well as pull-down of PDK2_{CPDK1}, PDK2_{CPDK3}, and PDK2_{CPDK4} on GST-LBD2 constructs, was carried out and analyzed in a similar fashion.

Isothermal Titration Calorimetry. Calorimetric measurements of the PDK2-LBD2 interaction were performed on a MicroCal VP-ITC microcalorimeter (MicroCal Inc., Northampton, MA) (21). Prior to the binding experiment, freshly made preparations of PDK2 and His₆-LBD2 were desalted on a PD-10 column (Amersham Biosciences Corp.) equilibrated in buffer B [20 mM potassium phosphate buffer (pH 7.5), 50 mM KCl, 10 mM MgCl₂, 5 mM dithiothreitol, and 2% (v/v) ethylene glycol]. Desalted proteins were passed through a 0.2 μ m filter and degassed by being stirred under vacuum before use. Experiments were performed at 30 \pm 0.2 °C. The sample cell was filled with a PDK2 solution (14–20 μ M), and while being stirred at 250 rpm, the system was allowed to equilibrate to an rms noise value of 0.008 J s⁻¹ before the start of the titration. The injection syringe was filled with His₆-LBD2 solution (420–580 μ M), and repeated 10 μ L injections were made. The calorimeter was calibrated using standard electrical pulses generated by the provided software. Calorimetric data were analyzed by integration of resultant peaks (ORIGIN software; MicroCal Software, Inc.). The heat change accompanying the addition of buffer to PDK2 and the heat of dilution of the ligand were subtracted from the raw data after correction for the injection signal of buffer into buffer. Binding parameters were obtained by nonlinear regression fitting to the isotherm. One set of sites, two sets of sites, and sequential binding site models were used to analyze the data.

As a control, we also carried out the titration experiments with ADP, which followed the same outline as that for His₆-LBD2. The injection syringe was filled with ADP (0.84 mM) solution made in buffer B. The ADP concentration was determined spectrophotometrically using the molar absorption coefficient at 260 nm (ϵ_{260}) of 15 400 M⁻¹ cm⁻¹.

Other Procedures. The activity of PDC was determined as described previously (12). SDS-PAGE was carried out according to the method of Laemmli (27). Protein concentrations were determined according to the Lowry method with bovine serum albumin as the standard (28). Concentrations of His₆-LBD2 were measured by the absorption at 280 nm using an absorption coefficient of 0.6994. Western blot analysis was performed as described previously using anti-His₆ tag antibodies (working dilution of 1:2000) purchased from Novagen (24). Immunoreactive bands were visualized following an ECL immunodetection procedure (Amersham Biosciences Corp.).

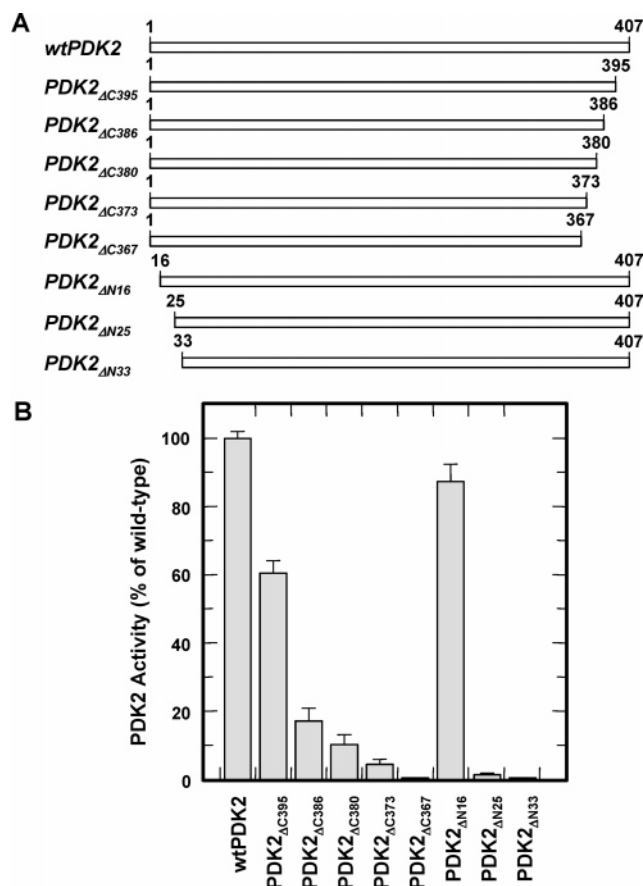


FIGURE 1: Enzymatic activities of truncated variants of PDK2. (A) Schematic illustrating the relationships between the truncated variants of PDK2. (B) Enzymatic activities of the truncated variants of PDK2 toward holo-PDC as a substrate. Data are expressed as the percent activity of wild-type PDK2.

RESULTS

Expression, Purification, and Activities of the Truncated Variants of PDK2. To investigate the role of amino- and carboxy-terminal tails of PDK2 in kinase function, series of deletions were introduced into the cDNA encoding the mature form of PDK2. As shown in Figure 1A, translation products of these cDNAs were lacking either 7 (PDK2 Δ N16), 16 (PDK2 Δ N25), or 24 (PDK2 Δ N33) amino acids at the amino terminus or 12 (PDK2 Δ C395), 21 (PDK2 Δ C386), 27 (PDK2 Δ C380), 34 (PDK2 Δ C373), or 40 (PDK2 Δ C367) amino acids at the carboxyl terminus. The cDNAs were expressed in bacteria under the control of the T₇ promoter. Analysis of the whole-cell extracts by Western blotting showed that all PDK2 variants were highly expressed in this system (data not shown). However, cellular fractionation revealed that PDK2 Δ N25, PDK2 Δ N33, and PDK2 Δ C367 proteins were largely present in the inclusion bodies. Their coexpression with molecular chaperonins, which greatly improved the yield of wild-type PDK2 (23), did not have an appreciable impact on the yields of soluble PDK2 Δ N25, PDK2 Δ N33, and PDK2 Δ C367. As described in Experimental Procedures, wild-type PDK2 and its variants were purified by metal affinity chromatography. On the basis of SDS-PAGE analysis, all purified proteins were of predicted size and did not undergo any proteolytic degradation (data not shown). The yields of all purified proteins except PDK2 Δ N25, PDK2 Δ N33, and PDK2 Δ C367 were comparable to that of wild-type PDK2. The yields of

PDK2 Δ N25, PDK2 Δ N33, and PDK2 Δ C367 were considerably lower, which is in agreement with their poor expression in soluble form. However, we were able to obtain a sufficient amount of each kinase for the initial characterization.

Analysis of PDK2 variants in the standard assay that utilizes the entire complex as a substrate revealed that truncation of either the amino- or carboxy-terminal tail greatly affects the kinase activity (Figure 1B). Sequential removal of the amino acids that form the carboxy-terminal tail was accompanied by a progressive decrease in activity. The activity of the most active variant, i.e., PDK2 Δ C395, was approximately 60% of that of the wild-type enzyme. The least active variant (PDK2 Δ C367) displayed only 1–2% of the activity of wild-type PDK2. Deletion of eight amino acids from the amino terminus of PDK2 (PDK2 Δ N16) caused just a slight decrease in kinase activity (approximately 15–18%). However, further truncations were associated with a great decrease in activity. As shown in Figure 1B, PDK2 Δ N25 and PDK2 Δ N33 variants displayed less than 1% of the activity of wild-type PDK2.

The activity of PDK strongly depends on protein–protein interactions (4). In particular, binding to E2 causes a more than 10-fold enhancement in the rate of phosphorylation (9). Thus, a decrease in the rates of phosphorylation observed in experiments described in Figure 1B could be due to either a decrease in kinase activity, impairment in the interaction with E2, or both. To examine these possibilities, we compared the rate of phosphorylation of E1 alone with the rates of phosphorylation of E1 in the presence of E2. It was found that truncation of the carboxyl tail of PDK2 was associated with a significant decrease in the ability of E2 to stimulate kinase activity. As shown in Figure 2A, E2-dependent enhancement of the phosphorylation rate decreased from approximately 10-fold for the wild-type PDK2 to less than 50% for PDK2 Δ C367. There was also a decrease in the phosphorylation rate of E1 alone, but it was less significant than that observed in the presence of E2. Among the variants carrying the truncations at the carboxyl terminus, PDK2 Δ C367 was the only kinase grossly deficient in its ability to phosphorylate free E1. Among the amino-terminal truncations, PDK2 Δ N16 exhibited just a slight decrease in E2-stimulated activity, indicating that the amino acid residues coming from the far amino terminus play little if any role in the E2-dependent regulation of PDK2. By contrast, both PDK2 Δ N25 and PDK2 Δ N33 exhibited a large decrease in the rate of phosphorylation regardless of whether free or E2-bound E1 was used as a substrate (data not shown). In conjunction with their poor solubility, these data suggest that these variants might have grossly altered conformations.

In general, E2 has a twofold effect on PDK. (a) It stimulates the kinase activity, and (b) it mediates the effects of NADH/NAD⁺ and acetyl-CoA/CoA (4). The results presented in Figure 2A indicate that the carboxy-terminal tail of PDK2 is critical for the increase in phosphorylation rate caused by the addition of E2. Moreover, the C-terminal tail also appears to be essential for the effects of NADH and acetyl-CoA as evidenced by the results in Figure 2B, showing that the shortening of the carboxyl terminus of PDK2 is associated with a progressive decrease in the effect of NADH and acetyl-CoA on kinase activity. Taken together, these data strongly suggest that the amino and carboxyl termini of PDK2 are important for the kinase activity. The

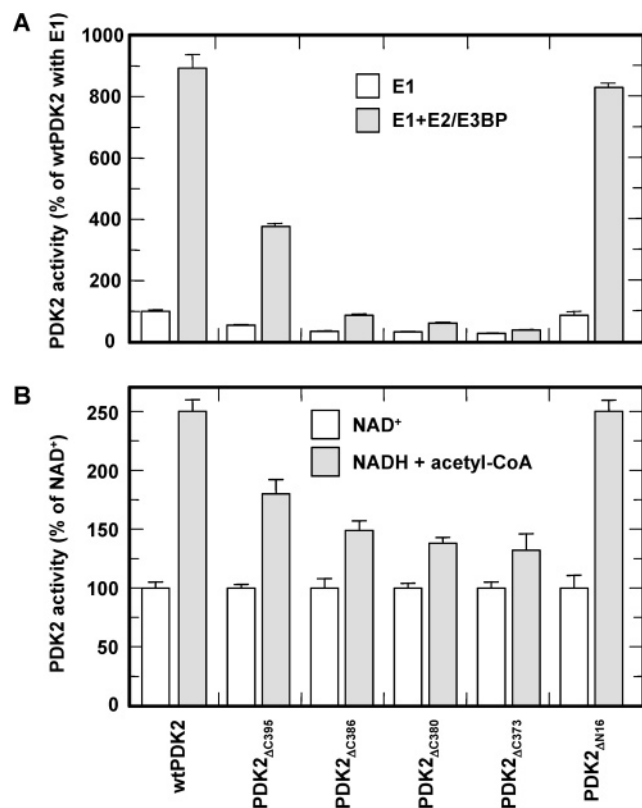


FIGURE 2: Effects of the E2-E3BP subcomplex and of NADH with acetyl-CoA on enzymatic activities of truncated variants of PDK2. (A) Regulation of kinase activities of PDK2 truncated variants by the E2-E3BP subcomplex. Activities toward the free E1 component are shown with white bars. Activities determined in the presence of the E2-E3BP subcomplex are shown with gray bars. Data are expressed as the percent activity of wild-type PDK2 toward the free E1 component. (B) Regulation of kinase activities of PDK2 variants by NADH with acetyl-CoA. NAD⁺ controls were made with the addition of a mixture of NAD⁺ and NADH (molar ratio of 200:1) to a final concentration of 0.8 mM (white bars). The effects of NADH and acetyl-CoA were determined with the addition of NADH and NAD⁺ in a mixture to final concentrations of 0.6 and 0.2 mM, respectively, and of acetyl-CoA to 50 μ M (gray bars). Effectors were added 30 s prior to ATP to allow for equilibration of the reactions catalyzed by E2 and E3 components. Data are expressed as the percent activity determined for NAD⁺ controls.

amino terminus is required for the overall ability of PDK2 to phosphorylate PDC, and clearly contribute to the proper folding of the kinase molecule. The carboxyl terminus appears to have a specialized role, being essential for the E2-dependent regulation of the phosphorylation reaction.

Interaction of Wild-Type PDK2 and Its Variants with Lipoyl-Bearing Domain(s) and PDC. As discussed in the introductory section, PDK is an integral part of PDC. Evidence presented by a number of laboratories strongly suggests that PDK is bound tightly to the transacetylase component of the complex with the lipoyl-bearing domain(s) being the primary docking sites for the kinase molecule (4). The transacetylase subcomplex has three types of lipoyl-bearing domains provided by E2 (LBD1 and LBD2) and by E3BP components (LBD3). To investigate the interactions between PDK2 and individual lipoyl-bearing domains, LBD1-LBD3 were expressed in bacteria as glutathione *S*-transferase fusions. The resulting constructs were used as bait to pull down the wild-type PDK2. As shown in Figure 3A, all three LBDs could bind PDK2 in the pull-down assay.

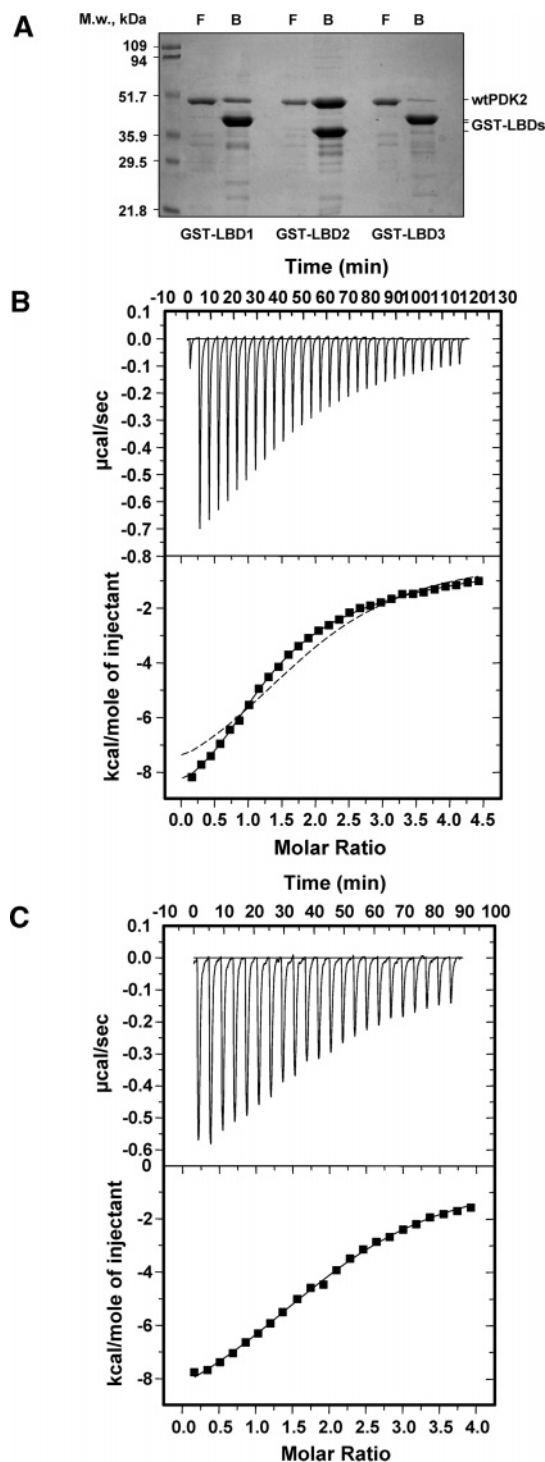


FIGURE 3: Binding of lipoyl-bearing domain(s) and of ADP by wild-type PDK2. (A) SDS-PAGE analysis of wild-type PDK2 pulled down using GST-based constructs of LBD1-LBD3. (B) Isothermal titration calorimetry of binding of LBD2 to wild-type PDK2. The top panel shows the calorimetric response as successive injections of LBD2 are added to the reaction cell containing PDK2. The bottom panel depicts the binding isotherm of the calorimetric titration shown in the top panel. The dashed line represents the best fit of the binding isotherm using a one-site model ($n = 2$, $K_A = 8.74 \times 10^4$, $\Delta H = -7.9$ kcal/mol). The solid line depicts the least-squares fit of the binding isotherm using a sequential binding sites model when $n = 2$. (C) Isothermal titration calorimetry of binding of ADP to wild-type PDK2. The top panel shows the calorimetric response as successive injections of ADP are added to the reaction cell containing PDK2. The bottom panel depicts the binding isotherm of the calorimetric titration shown in the top panel.

Table 1: Amounts of Wild-Type PDK2 Recovered in the LBD-Bound Form Using a GST-Based Pull-Down Assay^a

construct	bound kinase (percent of control) ^b
GST-LBD1	25 ± 4%
GST-LBD2 (control)	100 ± 9%
GST-LBD3	5 ± 1%

^a Pull-down experiments were carried out as described in Experimental Procedures. Coomassie R250-stained gels were analyzed and quantified using scanning densitometry. ^b Data are expressed as a percent of PDK2 bound to the GST-LBD2 construct. Results are means ± the standard deviation of six experiments.

Table 2: Dissociation Constants and Enthalpy Changes for Binding of ADP to Wild-Type PDK2^a

parameter	value ^b
<i>n</i> (stoichiometry)	2.0 ± 0.1
<i>K_D</i> (μM)	18.2 ± 1.4
Δ <i>H</i> (kcal/mol)	−11.8 ± 0.7

^a Dissociation constants and enthalpy changes for the binding of Mg-ADP to wild-type PDK2 were measured by isothermal titration calorimetry. ^b Results are expressed as means ± the standard deviation of four experiments conducted with freshly isolated preparations of wild-type PDK2.

The amount of PDK2 recovered in LBD-bound form decreased in the following order: LBD2 > LBD1 > LBD3 [the GST-LBD3 construct has just 5% of bound PDK2 relative to the GST-LBD2 construct (Table 1)]. This outcome is consistent with the data recently published by Hiromasa and Roche (29) and strongly suggests that LBD2 serves as the primary docking site for wild-type PDK2.

To obtain a quantitative measure of the strength of the interaction between PDK2 and LBD2, we employed isothermal titration calorimetry (ITC). Representative results of an isothermal titration calorimetric run in which PDK2 was titrated with LBD2 are shown in Figure 3B. The top portion of the figure shows the raw heat data from the run. The interaction was exothermic as evidenced by the negative peaks. The heat of LBD2 dilution was measured by titration of LBD2 into buffer alone and was subtracted from each binding titration curve. The integrated heats for each injection versus the molar ratio of LBD2 to PDK2 after subtraction of the heat of dilution of the ligand are illustrated in Figure 3B (bottom panel). Somewhat unexpectedly, our attempts to curve fit these data to a one-site model produced a rather poor fit (dashed line in the bottom panel of Figure 3B). This could indicate that either PDK2 follows a more complex LBD2 binding mechanism or a considerable percent of PDK2 in our preparations binds LBD2 poorly. Thus, for control purposes, we conducted ITC experiments in which ADP was titrated into wild-type PDK2 (Figure 3C). The heat released during the titration of ADP into a PDK2 solution exhibited good agreement with an ideal binding characterized by the presence of a single type of binding site and the lack of cooperativity in the interaction. On average, the fit of the ADP binding data resulted in a value for *n* (stoichiometry) of 2.0 per PDK2 dimer, a dissociation constant *K_D* of 18.2 μM, and an enthalpy change Δ*H*^o of −11.8 kcal/mol (Table 2). This suggests that all kinase molecules in PDK2 preparations used in these experiments were properly folded and could effectively bind nucleotide ligand, which, in turn, implies that LBD2 binding follows a mechanism more complex than a single-site model. Indeed, curve fitting of

Table 3: Dissociation Constants and Enthalpy Changes for Binding of LBD2 to Wild-Type PDK2^a

parameter	value ^b	parameter	value ^b
<i>K₁</i> (μM)	8.3 ± 2.3	<i>K₂</i> (μM)	93.3 ± 26.1
Δ <i>H</i> ₁ (kcal/mol)	−9.6 ± 0.6	Δ <i>H</i> ₂ (kcal/mol)	−31.6 ± 8.4

^a Dissociation constants and enthalpy changes for the binding of His₆-LBD2 to wild-type PDK2 were measured by isothermal titration calorimetry. ^b Results are expressed as means ± the standard deviation of five experiments conducted with freshly isolated preparations of wild-type PDK2.

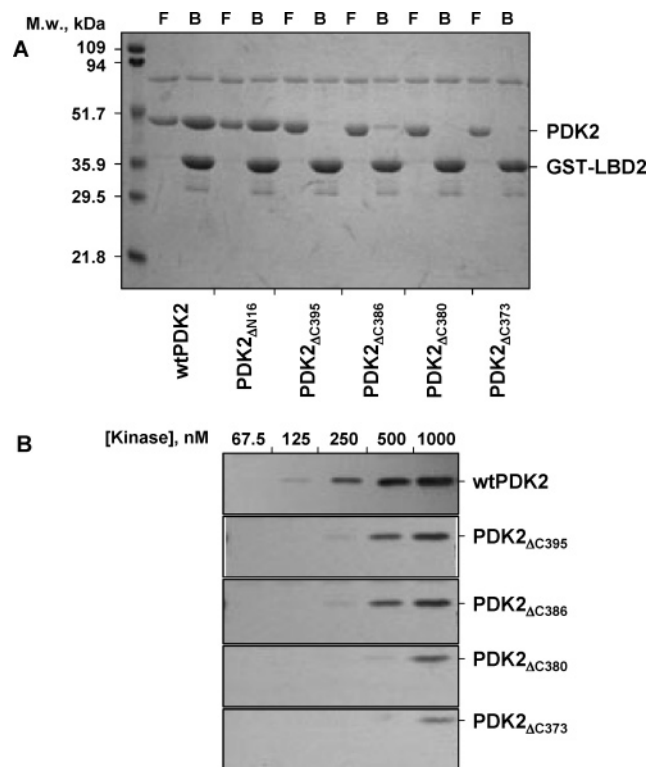


FIGURE 4: Binding of PDK2 and of its truncated variants to LBD2 and the E2-E3BP subcomplex. (A) SDS-PAGE analysis of wild-type PDK2 and its variants pulled down on the GST-LBD2 construct. (B) Binding of wild-type PDK2 and its variants to the E2-E3BP subcomplex. Bound kinase was visualized using Western blot analysis with monoclonal anti-His₆ tag antibodies.

LBD2 binding data to the model of two sequential binding sites produced a very good fit (solid line in the bottom panel of Figure 3B). For five preparations of PDK2 that were analyzed in this study, the average dissociation constants were $8.3 \pm 2.3 \mu\text{M}$ (*K_{D1}*) and $93.3 \pm 21.6 \mu\text{M}$ (*K_{D2}*) (Table 3). This outcome indicates that there might be an interaction between the LBD-binding sites in the PDK2 dimer.

It is feasible that the defects in E2-dependent regulation of PDK2 activity (Figures 1 and 2) associated with the truncation of its carboxyl terminus could come about as a result of the impaired LBD2 binding. To investigate this hypothesis, truncated variants were subjected to a GST-LBD2 pull-down assay. As shown in Figure 4A, all PDK2 variants truncated at the carboxyl terminus exhibited a greatly reduced affinity for LBD2, judging from the amount of kinase protein recovered in the LBD2-bound form. In agreement with this conclusion, PDK2_{ΔC395} and other PDK2 variants with truncations at the carboxyl terminus showed little if any interaction with LBD2 in ITC experiments (data not shown). Taken together, these data suggest that the

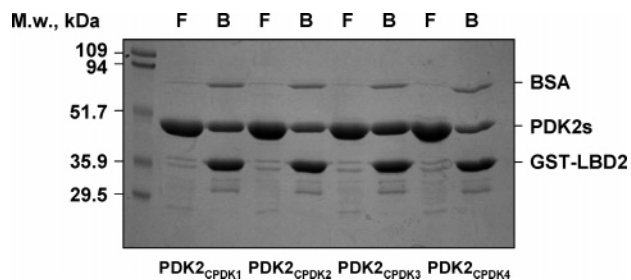


FIGURE 5: SDS-PAGE analysis of PDK2 chimeras pulled down using the GST-LBD2 construct.

carboxyl tail of PDK2 directly contributes to the LBD2-binding site of the kinase molecule.

Interestingly, it appeared that the deletion of the carboxyl terminus had a far greater impact on the interaction of PDK2 with LBD2 than on the kinase activity determined in the presence of E2 (Figure 2A). To explore this observation further, we characterized the binding of the respective PDK2 variants to the E2-E3BP subcomplex using gel-filtration chromatography. Figure 4B illustrates the amounts of each kinase recovered in the E2-E3BP-bound form obtained from the runs in which different amounts of kinase were chromatographed with the same amount of E2-E3BP subcomplex. It was found that the progressive deletion of the amino acids from the carboxyl terminus of PDK2 was accompanied by a decrease in the amount of kinase recovered in the complex-bound form and, qualitatively, was in a good agreement with the activity measurements.

Activities and Interactions with LBD2 of PDK2 Chimeras. Mammals have four isozymes of PDK that differ with respect to their tissue distribution, enzymatic activity, and regulation. At least three of these isozymes (PDK1-PDK3) were directly shown to exist in a complex-bound state (3, 5). All PDK isozymes have characteristic carboxyl tails that are markedly different in their amino acid composition (1, 2). This brings about an intriguing possibility that the unique properties of PDK isozymes are due at least in part to the differences in the sequences of their carboxyl tails. To investigate this hypothesis, we created chimeras in which the carboxyl tails derived from PDK1, PDK2, and PDK4 were attached to the kinase core derived from PDK2 (PDK2_{CPDK1}, PDK2_{CPDK3}, and PDK2_{CPDK4}, respectively). As described in Experimental Procedures, unique *StuI* sites were introduced by silent mutagenesis in the cDNAs encoding PDK1-PDK4. This created an exchange site for the swapping of carboxyl termini in the sequence corresponding to the invariant -Lys-Ala-Leu-Ser- consensus (see also Figure 7). The resulting mutagenized cDNAs for PDK1, PDK3, and PDK4 were used as a source of sequences encoding the carboxyl tails. The mutagenized cDNA of PDK2 was used as a source of sequence encoding the kinase core. Chimeric cDNAs were expressed in bacteria under the control of the T₇ promoter. Recombinant kinases were purified to near homogeneity by metal affinity chromatography. All chimeric kinases were expressed at the levels similar to that of wild-type PDK2 and did not display proteolytic degradation in SDS-PAGE analysis (data not shown).

The abilities of PDK2_{CPDK1}, PDK2_{CPDK3}, and PDK2_{CPDK4} to interact with LBD2 were first evaluated using a GST-LBD2 pull-down assay. As shown in Figure 5, it was found that all three chimeras could bind LBD2. On the basis of

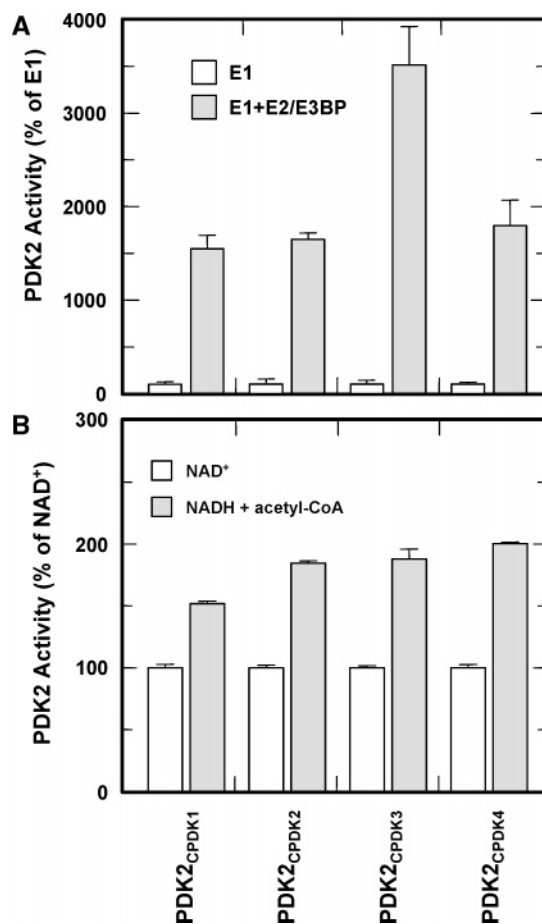


FIGURE 6: Effects of the E2-E3BP subcomplex and of NADH with acetyl-CoA on enzymatic activities of PDK2 chimeras. (A) Regulation of kinase activities of PDK2 chimeras by the E2-E3BP subcomplex. Activities toward the free E1 component are shown with white bars. Activities determined in the presence of the E2-E3BP subcomplex are shown with gray bars. Data are expressed as the percent activity toward the free E1 component. (B) Regulation of kinase activities of PDK2 chimeras by NADH with acetyl-CoA. NAD⁺ controls were made with the addition of a mixture of NAD⁺ and NADH (molar ratio of 200:1) to a final concentration of 0.8 mM (white bars). The effects of NADH and acetyl-CoA were determined with the addition of NADH and NAD⁺ in a mixture to final concentrations of 0.6 and 0.2 mM, respectively, and of acetyl-CoA to 50 μ M (gray bars). Effectors were added 30 s prior to ATP to allow for equilibration of the reactions catalyzed by E2 and E3 components. Data are expressed as the percent activity determined for the NAD⁺ control.

scanning densitometry, there was approximately 2 times more of PDK2_{CPDK3} chimera and approximately 30% less of PDK2_{CPDK4} chimera recovered in the LBD2-bound form (Table 4). The recovery of the PDK2_{CPDK1} chimera was similar to that of the control PDK2. In ITC experiments, the PDK2_{CPDK1} chimera bound LBD2 in a manner similar to that of the PDK2 control (Table 5). The PDK2_{CPDK3} chimera exhibited an approximately 3-fold greater affinity than the control, while the affinity of the PDK2_{CPDK4} chimera was slightly decreased, which is in an agreement with the outcome of pull-down experiments. Analysis of the respective kinases in phosphorylation assay revealed that PDK2_{CPDK3} displayed an approximately 2-fold greater activation in response to the addition of the E2-E3BP subcomplex (Figure 6A). By contrast, all chimeras exhibited a comparable response to NADH with acetyl-CoA (Figure 6B). Taken together, these data are consistent with the interpretation that

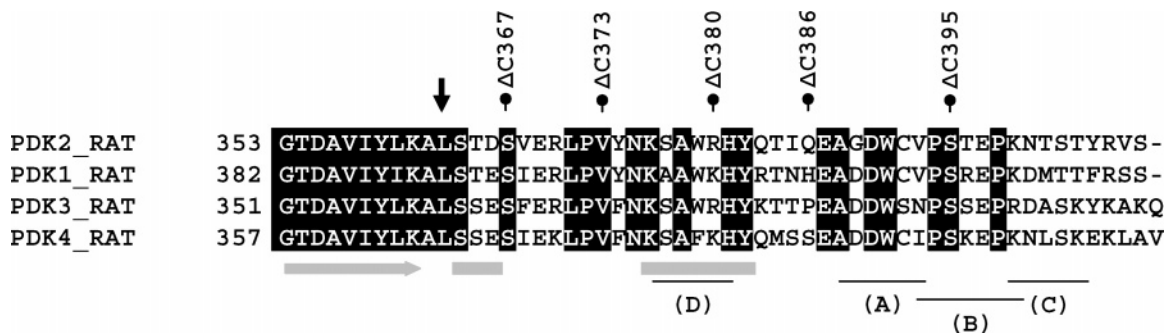


FIGURE 7: Sequence alignment of the carboxyl tails of rat PDKs. Four regions implicated in LBD2 binding (31), i.e., A–D, are indicated by black lines at the bottom of the alignment. Conserved amino acid residues are shown with inverted text. The elements of the secondary structure of PDK3 (31) are indicated by blocks (α -helices) and by block arrows (β strands) at the bottom of the alignment. Positions at which truncations were introduced into the sequence of rat PDK2 are shown at the top of the alignment. The position of the amino acid corresponding to the *StuI* exchange site that was used in carboxyl tail swapping experiments is indicated by an arrow at the top of the alignment.

Table 4: Amounts of Various PDK2 Chimeras Recovered in the LBD2-Bound Form Using a GST-Based Pull-Down Assay^a

kinase	bound kinase (percent of control) ^b
PDK2 _{CPDK1}	89 ± 5
PDK2 _{CPDK2} (control)	100 ± 9
PDK2 _{CPDK3}	185 ± 17
PDK2 _{CPDK4}	72 ± 8

^a Pull-down experiments were carried out as described in Experimental Procedures. Coomassie R250-stained gels were analyzed and quantified using scanning densitometry. ^b Data are expressed as a percent of PDK2_{CPDK2} bound to GST–LBD2 construct. Results are means ± the standard deviation of four to six experiments.

Table 5: Dissociation Constants for Binding of LBD2 to Various PDK2 Chimeras^a

	PDK2 _{CPDK1}	PDK2 _{CPDK3}	PDK2 _{CPDK4} ^b
K_1 (μ M)	9.6 ± 1.7	3.4 ± 0.1	13.2 ± 2.5
K_2 (μ M)	81.7 ± 3.1	36.7 ± 10.9	94.7 ± 23.9

^a Dissociation constants of His₆-LBD2 with PDK2 chimeras were measured by isothermal titration calorimetry. ^b Results are expressed as means ± the standard deviation of three to six determinations.

the carboxyl tail derived from any isozyme of PDK is sufficient for the support of LBD2 binding, activation by the E2–E3BP subcomplex, and the regulation of kinase activity by NADH and acetyl-CoA, although some of these responses appear to be isozyme-specific. The latter is particularly true for the carboxy-terminal tail of PDK3 that clearly confers a stronger binding to LBD2 and a greater response to the E2–E3BP subcomplex.

DISCUSSION

Besides the catalytic core that consists of K and B domains, the PDK molecule has relatively long amino and carboxyl tails (2, 20). To explore their role in kinase activity, we created a number of PDK2 variants truncated at the amino and carboxyl termini. Analysis of these variants revealed that the deletion of the first eight amino acids at the amino terminus had a weak effect on PDK2 activity and regulation, indicating that these amino acids are dispensable for kinase function. However, further deletions at the amino terminus were associated with a dramatic decrease in kinase activity accompanied by a loss of solubility. Even chaperonin-assisted folding failed to rescue these variants of PDK2, which is indicative of a gross change in kinase conformation. By

contrast, truncations at the carboxyl terminus had a relatively small effect on kinase activity toward the free E1 component, suggesting that the overall fold of the kinase domain was largely intact. The differences between these variants were apparent when their activities were assayed in the presence of the E2–E3BP subcomplex. In this assay, a progressive truncation of the carboxyl terminus was accompanied by a progressive decrease in the rate of phosphorylation, which is consistent with the interpretation that the carboxyl terminus of PDK2 is essential for the kinase activity in a complex-bound state. In agreement with this interpretation, the truncated forms of PDK2 exhibited a significantly reduced response toward NADH and acetyl-CoA, which is thought to be characteristic of a complex-bound kinase (14, 15).

It is generally believed that PDK2 is attached to PDC through the lipoyl-bearing domain(s) provided by the E2–E3BP subcomplex (LBD1–LBD3, respectively) (4). Although PDK2 can bind all three lipoyl-bearing domains, our data along with the results presented by others (3) strongly suggest that LBD2 is the most effective interactor. In ITC experiments, the PDK2 dimer displayed two LBD-binding sites differing with respect to their affinity for the lipoyl-bearing domain. On the basis of the available structural information, PDK2 in solution is a symmetric dimer (20). Consequently, there is no reason to assume that LBD-binding sites in the PDK2 molecule are nonidentical at the start. Therefore, it seems reasonable to propose that the LBD-binding sites in the PDK2 dimer are likely to be interacting. Furthermore, from the relationship between the dissociation constants (i.e., $K_{D1} < K_{D2}$), it appears that the binding of the first LBD2 hinders the binding of the second LBD2, yielding a negative cooperativity. It remains to be established whether this hindering effect exists in a complex-bound state. Importantly, we have found that the truncation of the carboxy-terminal tail of PDK2 is associated with a great decrease in the kinase's affinity for LBD2. This strongly suggests that the carboxyl terminus directly contributes to the structure of the LBD-binding site. This interpretation is also in agreement with the earlier data showing that the carboxyl-terminal fragment of PDK generated by trypsin treatment remains bound to PDC, whereas the amino-terminal fragment(s) is released into the medium (30).

By all criteria, the carboxyl tail of PDK2 appears to be indispensable for the interaction with the lipoyl-bearing domain(s). In mammals, there are four PDK isozymes, all

of which have the characteristic carboxyl tails that are somewhat different in the amino acid sequences (2). Several lines of evidence suggest that PDK isozymes are markedly different with respect to their ability to interact with the lipoyl-bearing domain(s) (3, 9). Here, we investigated the ability of the carboxyl tails derived from PDK1, PDK3, and PDK4 to support PDK2 activity and LBD2 binding. The results of the swapping experiment suggest that the carboxyl tail derived from any isozyme of PDK confers LBD2 binding. The chimeras carrying the carboxyl terminus of PDK3 displayed better LBD2 binding than wild-type PDK2, whereas the chimeras carrying the carboxyl terminus of PDK4 bound LBD2 slightly worse than the control kinase. This indicates that, at least in part, the differences in the amino acid sequences of the carboxyl tails account for the differences among PDK isozymes. However, it should be pointed out that the carboxyl tails derived from all isozymes are competent in supporting the interaction with LBD2, suggesting that the gross differences among PDK isozymes reflect the unique, yet to be identified features of each PDK core rather than the carboxyl tail.

While this paper was being reviewed, Kato and colleagues (31) published the first three-dimensional structure of isozyme PDK3 in a complex with LBD2. This structure revealed that the extended carboxyl tail from one PDK3 subunit crosses over to another subunit where it interacts with the bound LBD2 and accounts for almost 50% of the interface between LBD2 and PDK3. Furthermore, different parts of the carboxyl tail appear to make different contributions to the LBD-binding site (Figure 7). Amino acids from region A form an extensive hydrogen bond network with conserved amino acids coming from the neighboring PDK3 subunit, and amino acids from region B recognize the residues from LBD2 flanking the lipoyllysine. Amino acids from region C are integrated into the lipoyl-binding pocket, and finally, amino acids from region D contribute to the second interface with LBD2 in another PDK3 subunit. In agreement with these structural assignments, we have found that progressive truncation of the carboxyl tail causes a gradual loss of E2-dependent functions. This likely reflects different stages in degradation of the LBD-binding site caused by deletions, such as a loss of the side chains contributing to the lipoyl-binding pocket, a loss of the interactions with the amino acids flanking lipoyllysine, etc. (Figure 7). Interestingly, we have found that the deletion of the carboxyl terminus had a far greater impact on the interaction with LBD2 than on the interaction with the E2–E3BP subcomplex or on kinase activity determined in the presence of the E2–E3BP subcomplex. The rationale for this phenomenon is currently unknown. One possibility is that it reflects an unusual structure of the E2–E3BP subcomplex which presents the kinase molecule with numerous lipoyl-bearing domains [local concentration of up to 2–3 mM (4)]. This high local concentration of lipoyl-bearing domains on the surface of the E2–E3BP subcomplex might be great enough for the productive binding even if the affinity of PDK2 for LBD2 decreases more than 1 order of magnitude as a result of the deletion.

Despite the fact that the carboxyl tail accounts for the majority of sequence-specific interactions between PDK and the lipoyl-bearing domain (31), our swapping experiments clearly show that the specificity of interaction between kinase

and LBD2 largely depends on the structural elements of the PDK core. In this respect, the amino acid residues of the B domain are of particular interest because, according to the structural data, the B domain of PDK3 contributes to the second binding interface with LBD2 (31). In this study, we attempted to investigate the role of the B domain in LBD2 binding by introducing several deletions into the amino terminus of PDK2. On the basis of the structural information (31), the largest of the deletions characterized in this study (PDK2_{ΔN33}) removed a significant portion of the second interface, including some of the amino acid residues lining the lipoyllysine-binding pocket. Unfortunately, this approach proved to be less informative because of the considerable problems associated with the folding of the majority of PDK2 variants carrying the amino-terminal truncations. Thus, although the B domain clearly provides a structural determinant contributing to LBD2 binding, its functional significance remains enigmatic. The functional role of the B domain in LBD2 binding will be undoubtedly addressed in future studies relying on structure-guided mutagenesis, which became possible after the structure of the PDK3–LBD2 complex had been determined (31).

REFERENCES

1. Gudi, R., Bowker-Kinley, M. M., Kedishvili, N. Y., Zhao, Y., and Popov, K. M. (1995) Diversity of the pyruvate dehydrogenase kinase gene family in humans, *J. Biol. Chem.* 270, 28989–28994.
2. Bowker-Kinley, M. M., Davis, W. I., Wu, P., Harris, R. A., and Popov, K. M. (1998) Evidence for existence of tissue-specific regulation of the mammalian pyruvate dehydrogenase complex, *Biochem. J.* 329, 191–196.
3. Baker, J. C., Yan, X., Peng, T., Kasten, S., and Roche, T. E. (2000) Marked differences between two isoforms of human pyruvate dehydrogenase kinase, *J. Biol. Chem.* 275, 15773–15781.
4. Roche, T. E., Baker, J. C., Yan, X., Hiromasa, Y., Gong, X., Peng, T., Dong, J., Turkan, A., and Kasten, S. A. (2001) Distinct regulatory properties of pyruvate dehydrogenase kinase and phosphatase isoforms, *Prog. Nucleic Acid Res. Mol. Biol.* 70, 33–75.
5. Popov, K. M., Shimomura, Y., and Harris, R. A. (1991) Purification and comparative study of the kinases specific for branched chain α -ketoacid dehydrogenase and pyruvate dehydrogenase, *Protein Expression Purif.* 2, 278–286.
6. Patel, M. S., and Roche, T. E. (1990) Molecular biology and biochemistry of pyruvate dehydrogenase complexes, *FASEB J.* 4, 3224–3233.
7. Ravindran, S., Radke, G. A., Guest, J. R., and Roche, T. E. (1996) Lipoyl domain-based mechanism for the integrated feedback control of the pyruvate dehydrogenase complex by enhancement of pyruvate dehydrogenase kinase activity, *J. Biol. Chem.* 271, 653–662.
8. Yang, D., Gong, X., Yakhnin, A., and Roche, T. E. (1998) Requirements for the adaptor protein role of dihydrolipoyl acetyltransferase in the up-regulated function of the pyruvate dehydrogenase kinase and pyruvate dehydrogenase phosphatase, *J. Biol. Chem.* 273, 14130–14137.
9. Tuganova, A., Boulatnikov, I., and Popov, K. M. (2002) Interaction between the individual isoenzymes of pyruvate dehydrogenase kinase and the inner lipoyl-bearing domain of transacetylase component of pyruvate dehydrogenase complex, *Biochem. J.* 366, 129–136.
10. Zhou, Z. H., McCarthy, D. B., O'Connor, C. M., Reed, L. J., and Stoops, J. K. (2001) The remarkable structural and functional organization of the eukaryotic pyruvate dehydrogenase complexes, *Proc. Natl. Acad. Sci. U.S.A.* 98, 14802–14807.
11. Coppel, R. L., McNeilage, L. J., Surh, C. D., Van de Water, J., Spithill, T. W., Whittingham, S., and Gershwin, M. E. (1988) Primary structure of the human M2 mitochondrial autoantigen of primary biliary cirrhosis: Dihydrolipoamide acetyltransferase, *Proc. Natl. Acad. Sci. U.S.A.* 85, 7317–7321.
12. Harris, R. A., Bowker-Kinley, M. M., Wu, P., Jeng, J., and Popov, K. M. (1997) Dihydrolipoamide dehydrogenase-binding protein

- of the human pyruvate dehydrogenase complex. DNA-derived amino acid sequence, expression, and reconstitution of the pyruvate dehydrogenase complex, *J. Biol. Chem.* 272, 19746–19751.
13. Liu, S., Baker, J. C., and Roche, T. E. (1995) Binding of the pyruvate dehydrogenase kinase to recombinant constructs containing the inner lipoyl domain of the dihydrolipoyl acetyltransferase component, *J. Biol. Chem.* 270, 793–800.
14. Cooper, R. H., Randle, P. J., and Denton, R. M. (1975) Stimulation of phosphorylation and inactivation of pyruvate dehydrogenase by physiological inhibitors of the pyruvate dehydrogenase reaction, *Nature* 257, 808–809.
15. Cate, R. L., and Roche, T. E. (1978) A unifying mechanism for stimulation of mammalian pyruvate dehydrogenase(a) kinase by reduced nicotinamide adenine dinucleotide, dihydrolipoamide, acetyl coenzyme A, or pyruvate, *J. Biol. Chem.* 253, 496–503.
16. Linn, T. C., Pettit, F. H., and Reed, L. J. (1969) α -keto acid dehydrogenase complexes. X. Regulation of the activity of the pyruvate dehydrogenase complex from beef kidney mitochondria by phosphorylation and dephosphorylation, *Biochemistry* 62, 234–241.
17. Ono, K., Radke, G. A., Roche, T. E., and Rahmatullah, M. (1993) Partial activation of the pyruvate dehydrogenase kinase by the lipoyl domain region of E2 and interchange of the kinase between lipoyl domain regions, *J. Biol. Chem.* 268, 26135–26143.
18. Kolobova, E., Tuganova, A., Boulatnikov, I., and Popov, K. M. (2001) Regulation of pyruvate dehydrogenase activity through phosphorylation at multiple sites, *Biochem. J.* 358, 69–77.
19. Korotchikina, L. G., and Patel, M. S. (2001) Site specificity of four pyruvate dehydrogenase kinase isoenzymes toward the three phosphorylation sites of human pyruvate dehydrogenase, *J. Biol. Chem.* 276, 37223–37229.
20. Steussy, C. N., Popov, K. M., Bowker-Kinley, M. M., Sloan, R. B., Harris, R. A., and Hamilton, J. A. (2001) Structure of pyruvate dehydrogenase kinase. Novel folding pattern for a serine protein kinase, *J. Biol. Chem.* 276, 37443–37450.
21. Tuganova, A., and Popov, K. M. (2005) Role of protein–protein interactions in the regulation of pyruvate dehydrogenase kinase activity, *Biochem. J.* 387, 147–153.
22. Sanger, F., Nicklen, S., and Coulson, A. R. (1977) DNA sequencing with chain-terminating inhibitors, *Proc. Natl. Acad. Sci. U.S.A.* 74, 5463–5467.
23. Popov, K. M., Kedishvili, N. Y., Zhao, Y., Gudi, R., and Harris, R. A. (1994) Molecular cloning of the p45 subunit of pyruvate dehydrogenase kinase, *J. Biol. Chem.* 269, 29720–29724.
24. Kunkel, T. A., Roberts, J. D., and Zakour, R. A. (1987) Rapid and efficient site-specific mutagenesis without phenotypic selection, *Methods Enzymol.* 154, 367–382.
25. Quinn, J., Diamond, A. G., Masters, A. K., Brookfield, D. E., Wallis, N. G., and Yeaman, S. J. (1993) Expression and lipoylation in *Escherichia coli* of the inner lipoyl domain of the E2 component of the human pyruvate dehydrogenase complex, *Biochem. J.* 289, 81–85.
26. Boulatnikov, I., and Popov, K. M. (2003) Formation of functional heterodimers by isozymes 1 and 2 of pyruvate dehydrogenase kinase, *Biochim. Biophys. Acta* 1645, 183–192.
27. Laemmli, U. K. (1970) Cleavage of structural proteins during the assembly of the head of bacteriophage T4, *Nature* 227, 680–685.
28. Lowry, O. H., Rosebrough, N. J., Farr, A. L., and Randall, R. J. (1951) Protein measurement with the folin phenol reagent, *J. Biol. Chem.* 193, 265–275.
29. Hiromasa, Y., and Roche, T. E. (2003) Facilitated interaction between the pyruvate dehydrogenase kinase isoform 2 and the dihydrolipoyl acetyltransferase, *J. Biol. Chem.* 278, 33681–33693.
30. Chen, W., Komuniecki, P. R., and Komuniecki, R. (1999) Nematode pyruvate dehydrogenase kinases: Role of the C-terminus in binding to the dihydrolipoyl transacetylase core of the pyruvate dehydrogenase complex, *Biochem. J.* 339, 103–109.
31. Kato, M., Chuang, J. L., Tso, S.-C., Wynn, R. M., and Chuang, D. T. (2005) Crystal structure of pyruvate dehydrogenase kinase 3 bound to lipoyl domain 2 of human pyruvate dehydrogenase complex, *EMBO J.* 24, 1763–1774.

BI0505868